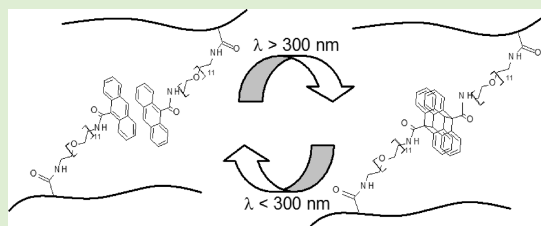


# Photoresponsive PEG-Anthracene Grafted Hyaluronan as a Controlled-Delivery Biomaterial

Laura A. Wells, Stephanie Furukawa, and Heather Sheardown\*

Department of Chemical Engineering and School of Biomedical Engineering McMaster University, Hamilton, Ontario, Canada

**ABSTRACT:** Ophthalmic drug delivery to the posterior segment of the eye could benefit from a responsive controlled drug delivery system with light or laser inducible changes. For example, the delivery of age-related macular degeneration drugs requires invasive monthly injections making long-term photoresponsive drug delivery a desirable option. The feasibility of this may be facilitated by both the transparency of the eye and the advanced technology in ophthalmic lasers. Hyaluronic acid photogels that are compatible with retinal pigment epithelial cell lines are shown here to deliver a variety of small and large model drugs over the long term (months). Varying UV exposures resulted in decreases/increases or the turning off and on of delivery, potentially allowing the therapy to be tailored to suit the patient and the disease.



## INTRODUCTION

The delivery rate of therapeutics can be adjusted using responsive controlled drug delivery devices to suit the natural progression of chronic diseases over years and to tailor delivery to the individual needs of the patients. The modification of polymer systems with molecules that respond to internal or external stimuli such as temperature, pH, or light can introduce controllable property changes<sup>1</sup> to alter drug releasing dosing profiles in pulsatile (on/off) or incremental (increase/decrease) fashions over the lifetime of a delivery device.

The potential benefits of responsive controlled delivery systems are obvious in ophthalmic drug delivery for the treatment of posterior segment eye diseases such as wet age related macular degeneration (wet AMD) and diabetic retinopathy. Both diseases can result in significant vision loss. However, disease progression can potentially be arrested or reversed with new long-term treatments. Many new vascular endothelial growth factor (VEGF)-blocker drugs on the market have been shown to effectively suppress the disease pathology.<sup>2</sup> However, delivery to the retina remains a challenge. Topical eye-drop therapies deliver insufficient drug to the posterior segment with only 5% drug penetration into the eye.<sup>3,4</sup> Systemic drug delivery can result in side effects to nontarget organs and these drugs have very little capability to diffuse through the low permeability vessels of the blood–retinal barrier to reach the target site.<sup>5</sup> The most effective technique for retinal drug delivery is intravitreal injections which, while effective, must be repeated approximately monthly for the treatment of wet AMD. This injection frequency is associated with injection-related side effects, low patient compliance, and high health care costs.<sup>6–8</sup> Controlled drug delivery devices for macular diseases that can deliver on the order of years have been well recognized to potentially alleviate these injection issues.<sup>9–11</sup> Furthermore, studies have suggested there are potential cost benefits with sustained visual improvements associated with altered AMD drug dose regimens based on monitoring with

optical coherence tomography.<sup>12,13</sup> Therefore, controlled release of drugs from smart materials that can incrementally alter released doses with stimuli over lengthy periods would present new methods to improve and optimize AMD treatments with VEGF-blocking agents.

Smart/responsive drug delivery systems made from polymers modified with photoisomerizing or photodimerizing groups have minimal side products and require no photosensitizers, eliminating the toxicity risks associated with leachable molecules and producing potentially highly biocompatible biomaterials for In Vivo applications.<sup>1</sup> In addition, site-specific, stimuli-responsive delivery would reduce side effects in comparison to photodynamic therapy for AMD, which requires systemic delivery of molecules followed by their activation via lasers.<sup>11</sup> Because individual photosensitive molecules in photoisomerizing or photodimerizing systems must absorb light to isomerize or dimerize,<sup>14,15</sup> in contrast to photopolymerization, which is characterized by absorption of light by initiators followed by propagation,<sup>16</sup> incremental changes may be achieved with higher exposures leading to additional photoreactions and vice versa. In addition, the presence of more photosensitive molecules should increase the overall magnitude of these changes.

The vitreous humor, a clear gel that fills the back of the eye, consists largely of water (>98%) with collagen and hyaluronan (HA).<sup>17</sup> Most retinal drug delivery devices would come into contact with and deliver drugs into the vitreous humor so gel devices synthesized with HA would presumably be highly compatible and would slowly degrade through the action of low levels of native enzymes. Previous studies by Wells and Sheardown (2011) focused on the synthesis of anthracene-containing hydrogels. These materials were synthesized via the

Received: October 15, 2010

Revised: January 24, 2011

Published: March 14, 2011

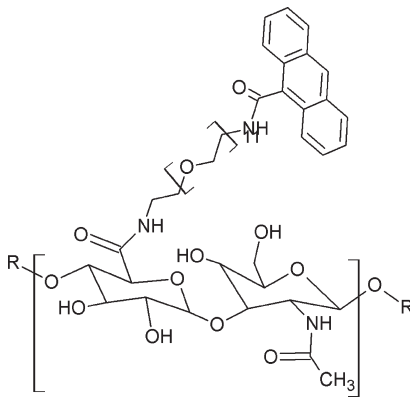


**Figure 1.** PEG-anthracene grafted onto HA.

grafting of polyethylene glycol (PEG)-bound anthracene groups along the backbone of HA, as illustrated in Figure 1.<sup>18</sup> Anthracene dimerizes at ultraviolet (UV) wavelengths over 300 nm and dedimerizes/dissociates at UV wavelengths under 300 nm,<sup>14</sup> creating a switchable mechanism that cross-links HA upon dimerization of anthracene due to the joining of grafted PEG chains and de-cross-links HA upon dedimerization of the anthracene groups.

Herein we explored HA photogel properties with the delivery of various compounds of high and low molecular weight with varying light exposures. Changes in release with light were consistently observed with both small and large model drug compounds that are representative of small anti-inflammatory steroids and larger anti-VEGF AMD drugs for retinal treatments. Altering the dose of 365 nm UV light was shown to cause incremental changes in release and the addition of anthracene-containing star-PEG can modify the sensitivity. Growth of retinal pigment epithelial cells with the photogels and degradation products showed high compatibility with similar cell viability as controls.

## METHODS

**Materials.** Sodium hyaluronate of 132.3 kDa was purchased from Life-Core Biomedical (Chaska, MN). PEG-diamine (*O,O'*-bis(2-aminoethyl) octadecaethylene glycol), Boc-PEG-amine (*O*-(2-aminoethyl)-*O'*-[2-(Boc-amino)ethyl]decaethylene glycol), 1-ethyl-(dimethylaminopropyl) carbodiimide hydrochloride (EDC), *N*-hydroxysuccinimide (NHS), ninhydrin assay reagent, MTT reagent (3-[4,5-dimethylthiazol-2-yl]-2,5-diphenyl tetrazolium bromide), proteins (myoglobin, lysozyme, and bovine serum albumin), small molecules (Coomassie Blue, Fast Green and dextran), and other reagents were purchased from Sigma-Aldrich (Oakville, ON). Anthracene-9-carboxylic acid was from Alfa Aesar (CA) and star-PEG-anthracene (four arm, with a pentaerythritol core, 9500 Da) was purchased from Polymer Source (Quebec). A 10 mW/cm<sup>2</sup> Curzone II lamp from CON-TROL-CURE (Chicago, IL; 400 W, 120 VAC, 60 Hz, 8 A max) was used for 365 nm UV exposures and an excimer laser (krypton fluoride, at 58 mJ/cm<sup>2</sup> and 5 Hz) was used for 248 nm exposures. Human retinal pigment epithelial (RPE) cells were from ATCC (Manassas, VA) with media and supplements from Invitrogen (Burlington ON).

**Photogel Synthesis.** As previously described in detail in Wells et al. (2011),<sup>18</sup> amine-terminated PEG-anthracene molecules were synthesized using carbodiimide chemistry between Boc-PEG-amine ( $n = 11$ ; 200 mg) and anthracene-9-carboxylic acid (288 mg) using EDC (268 mg) in dry dichloromethane (20 mL) under nitrogen. This was followed by removal of the Boc protecting group in DCM (16 mL) with

trifluoracetic acid (2 mL) and the scavenger triisopropylsilane (4 mL) then subsequent purification.<sup>18</sup>

Photogels were then synthesized in MES buffer containing 0.1 M 4-morpholinoethanesulfonic acid and 0.5 M sodium chloride (pH = 6) by mixing 6% HA with EDC/NHS solution and PEG-anthracene with varying HA/PEG-anthracene ratios at 4 °C for 72 h. The resulting photogels were then punched into disks and soaked in deionized water to remove impurities.<sup>18</sup> To optimize the properties of the HA photogels and control PEG hydrogels, varying molar ratios of PEG-anthracene to HA carboxyl groups were reacted and monitored for grafting efficiency. The photo-cross-linking ability of 0.8:1 versus 1:1 gels were used to test which photogels showed the highest photosensitivity.

To make 1:1 grafted photogels used in the release studies, 1 mL of 6% HA was mixed with 0.353 mL of EDC/NHS solution (191.6 mg/mL EDC and 57.5 mg/mL NHS) and 0.443 mL PEG-anthracene solution (300 mg/mL with 1N NaOH to pH = 6). The solution was allowed to react between glass plates with a 1 mm slide spacer and in the dark at 4 °C overnight. Control-PEG-hydrogels consisting of HA cross-linked with PEG chains were synthesized as nonphotoresponsive control gels for release studies. Control-PEG-hydrogels had less PEG added (0.443 mL of 180 mg/mL PEG-diamine of  $n = 20$  plus HCl to pH = 6) because both ends will react to the HA.

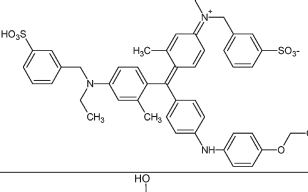
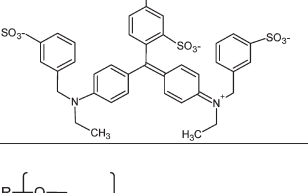
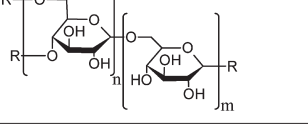
Star-PEG-anthracene was incorporated into some gels to increase the number of anthracene groups with a goal of increasing the photosensitivity of the gels. Star-PEG-anthracene was dissolved into the initial PEG-anthracene solution followed by mixing with EDC/NHS and 6% HA. Star-containing photogels additionally had 40.6 mg of star-PEG-anthracene per mL of 6% HA in an anthracene molar ratio of grafted PEG-anthracene to star-PEG-anthracene of 10:1.

**Ninhydrin Assay to Monitor Grafting.** The ninhydrin assay detects primary amine groups on unbound PEG-diamine and PEG-anthracene through the conversion of ninhydrin to Ruhemann's purple. By testing the gel soaking solutions and gels, unbound PEG can be detected and concentrations determined by a calibration curve of glycine. Gels soaked in 1 mL of water and 1 mL soaking solutions from their purification were mixed with 0.5 mL of reagent and heated in an oil bath at 100 °C for 10 min. After cooling at room temperature, 2.5 mL of 95% ethanol was added to dilute the samples followed by detection of Ruhemann's purple by spectrophotometric measurements of solution adsorption at 595 nm in a microplate reader. The unbound PEG-anthracene or PEG-diamine was compared to the amounts added during synthesis to determine the efficiency of the reaction (unbound–bound/bound) and the actual grafting ratios of the resulting gels (moles of PEG-anthracene per mole of HA polymer carboxyl groups).

**Release Studies.** To investigate drug release from and diffusion properties of the gels, model drug compounds were loaded and released from photogels with and without UV treatment. Air-dried gel disks (1.45 ± 0.03 mg) were loaded by soaking in 1 mL of 0.5 mg/mL solutions of the model compounds in PBS for 24 h. The photogel disks (22.2 ± 5 mg) were then rinsed and placed in PBS at 37 °C in a shaking water bath with periodic changes in the PBS soaking medium. This medium was sampled and tested over time to obtain release profiles. At 1.5 h, certain sets of gels were irradiated in 1 mL of PBS with 365 nm light in a UV chamber and compared to controls with no UV light exposure. Some gels in protein release studies were also exposed to 248 nm excimer laser (58 mJ/cm<sup>2</sup> and 5 Hz) on slides after approximately 1000 h of release and release results were compared to controls with no UV light and gels that were exposed to exclusively 365 nm light.

Three different small molecules, Coomassie Blue (854 Da), Fast Green (765.9 Da), and dextran (1000 Da), were loaded into and released from the HA photogels (Table 1). Coomassie blue and Fast Green were detected spectrophotometrically at 595 and 630 nm, respectively. Dextran was detected spectrophotometrically at 405 nm after precipitation for 5 min with ethanol in a sample/ethanol volumetric

**Table 1. Properties of the Different Small and Large Model Compounds Used in the Release Studies**

Small Model Compounds	Name	Molecular Weight	Structure
Coomassie Blue		854 Da	
Fast Green		766 Da	
Dextran		1000 Da	
Large Model Compounds	Name	Molecular Weight	Isoelectric Point
Myoglobin		17,600 Da	7.3, minor 6.8
Lysozyme		14,400 Da	9.3
BSA		67,000 Da	4.9

ratio of 1:2. Loading of the small molecules was determined by measuring the amounts of unloaded compounds remaining in the soaking solution.

Three proteins of varying molecular weight and isoelectric points (pI) were used in the release studies as model compounds (Table 1). Release of lysozyme, bovine serum albumin (BSA) and myoglobin was detected using the Bradford assay. Loading was defined as the average amount of protein completely released by the control (no UV) photogels that release and degrade quickly.

**Effective Cross-Linking Density.** Effective cross-linking densities were used to assess possible cross-linking from interactions of the model compounds with the photogel bulk materials or the anthracene. The effective cross-linking density ( $\nu_e$ ) was determined by dividing the polymer density ( $\rho_p$ ) of the average molecular weight between cross-links ( $M_c$ ) as per eq 1.

$$\nu_e = \frac{\rho_p}{M_c} \quad (1)$$

$M_c$  is determined using an adapted version of the Flory–Rehner equation by Bray and Merrill (eq 2) for hydrogels cross-linked in solution.<sup>19–21</sup> In eq 2,  $v$  is the specific volume of dry polymer (HA = 0.814 cm<sup>3</sup>/g<sup>22</sup> and PEG = 0.89 cm<sup>3</sup>/g for PEG<sup>23</sup>),  $v_{2,s}$  is the volumetric polymer fraction at maximum swelling calculated from swelling in PBS,  $v_{2,r}$  is the volumetric polymer fraction in a relaxed state calculated from synthesis masses,  $V_1$  is the molar volume of solvent (18 mol/cm<sup>3</sup>),  $\chi$  is the Flory polymer–solvent interaction parameter (approximately 0.473 for HA<sup>22</sup> and PEG<sup>23</sup>), and  $M_n$  is the number average molecular weight of the polymer.

$$\frac{1}{M_c} = \frac{2}{M_n} - \frac{(v/V_1)[\ln(1 - v_{2,s}) + v_{2,s} + \chi(v_{2,s})^2]}{v_{2,r}[(v_{2,s}/v_{2,r})^{1/3} - 0.5(v_{2,s}/v_{2,r})]} \quad (2)$$

**Diffusion Calculations.** Diffusion exponents describe the diffusion mechanism of molecules and diffusion coefficients the speed of the molecules and are a method of directly comparing the effect of different

molecules and exposures on the photogel systems. The release mechanisms were determined by calculating diffusion exponents using the relationship in eq 3 by linear regression of the natural logarithms of release data from 20 h after UV treatments until 500 h.  $M_t$  and  $M_\infty$  are the amount of drug released at time  $t$  and at infinite time,  $k$  is a constant dependent on the system, and  $n$  is the diffusion exponent. The diffusion exponent is indicative of the type of release. The gel disks were treated as slabs since their diameters are over 4 times their thickness.<sup>24,25</sup> For Fickian release ( $n \leq 0.5$ ), during an early time when  $M_t/M_\infty \leq 0.6$ , diffusion coefficients can be calculated using the Ritter and Peppas model shown in eq 4 for controlled release of polymeric devices,<sup>26</sup> where  $l$  is the thickness of the slab and  $D$  is the diffusion coefficient. Regression on the natural logarithms of release data from various photogels were used to determine their diffusion coefficients.

$$\frac{M_t}{M_\infty} = kt^n \quad (3)$$

$$\frac{M_t}{M_\infty} = 4 \left[ \frac{Dt}{\pi l^2} \right]^{1/2} \quad (4)$$

**Degradation Studies.** Hydrolytic and de-cross-linking driven degradation of the gels was monitored by soaking disks in 1 mL of phosphate buffered saline (PBS) at 37 °C with regular changes of the buffer until disks were no longer visible. Enzymatic degradation of HA by hyaluronidase (bovine testes) was monitored by placing the disks in 0.5 mL buffer containing 100 units of hyaluronidase per mL at 37 °C with regular solution changes to ensure maintenance of the enzyme activity. The buffer was prepared using 3.871 g of sodium citrate, 10.647 g of disodium hydrogen phosphate, and 4.383 g of sodium chloride in 500 mL of water with pH adjusted to 6.3 with 1 N NaOH/1 N HCl to promote enzyme function.

**Photogel Cytocompatibility with Retinal Cells.** Human retinal pigment epithelial (RPE) cells were grown in Dulbecco's modified Eagle's F12 medium (DMEM-F12) containing 5% fetal bovine serum, 1% L-glutamine, and 0.8% sodium bicarbonate and incubated at 37 °C with 5% carbon dioxide and 95% air. After growth with PEG-anthracene, HA, photogels, or degradation products, the cell populations were assessed using the MTT assay (Sigma-Aldrich), which monitors mitochondrial function by conversion of MTT to purple formazan by enzymes. A 0.4 mg/mL solution of MTT in medium was added to cells and they were incubated for 4 h followed by the dissolution of formazan precipitate into DMSO, which was measured spectrophotometrically at 595 and 700 nm. PEG-anthracene solutions were sterile filtered and gels were sterilized with ethanol after synthesis to avoid UV sterilization, which would induce premature dimerization.

Solutions of PEG-anthracene in medium were used to evaluate direct effects of the molecules on cell viability and growth. Varying densities of cells (17000–68000 cells/well) were grown for 24 h on a 48-well plate, at which time varying concentrations of PEG-anthracene were added. The MTT assay was used to evaluate cell viability 3 or 7 days after the addition of PEG-anthracene to the cell media. Solutions of HA (0–0.1 mg/mL in medium) were added to RPE cells 24 h after seeding at 120000 cells/well in a 48-well plate and tested with the MTT assay to assess the effect HA may have on cell growth.

Cells were grown with gels separated by an insert to test for the effect byproduct may have on RPE cell growth and respiration. Gels were sterilized with a 2 h ethanol soak followed by sterile air drying for 16 h and a medium soak for 2 h. A total of 24 h after seeding of 300000 cells/well in a 24-well plate, cell inserts (low density, 1.0 μm pore-size) with gels were introduced and cells were grown for an additional 3 or 7 days then tested with the MTT assay.

**Table 2.** Grafting Efficiency and Resulting Molar Ratios of PEG-Anthracene to HA Carboxyl Groups in the Synthesis of Photogels and Control PEG Hydrogels

procedural ratio of NH <sub>2</sub> /COOH	photogels (grafting of NH <sub>2</sub> -PEG-anthracene)		control PEG hydrogels (grafting of PEG-diamine)	
	grafting efficiency	ratio grafted/percent grafting	grafting efficiency	ratio grafted/Percent grafting
1.2:1	96%	1:1/100%	86%	1:1/100%
1.1:1	87%	0.94:1/94%	83%	0.9:1/90%
0.95:1	83%	0.8:1/80%	87%	0.83:1/83%
0.9:1	86%	0.76:1/76%	83%	0.74:1/74%
0.83:1	87%	0.72:1/72%	81%	0.68:1/68%

Long-term degradation products were grown with cells to test the long-term effects the gels may have as they degrade. Sterilized gels in 2 mL of medium and medium alone (with no gels) were put in an incubator for 45 days. Low concentrations of degradation products (0.2 mL of the soaking medium with 0.4 mL of fresh medium) or high concentrations of degradation products (0.6 mL of soaking medium) were added to cells that were previously seeded at 120000 cells/well (48 well plate) and grown for 24 h. Controls of 0.6 mL of fresh medium were used to verify the technique. Cell growth and viability 3 days later was then assessed with the MTT assay.

## RESULTS AND DISCUSSION

**Gel Synthesis.** The grafting of PEG-anthracene to HA provides a photoinduced cross-linking mechanism with anthracene dimerization causing the grafted PEG groups to join effectively causing cross-linking of the HA chains. Varying ratios of PEG-anthracene or PEG-diamine and HA (available carboxyl groups) were added into the reaction mixture to observe the resulting gel properties and grafting efficiencies in the synthesis of photogels and control-PEG-hydrogels (Table 2). Increases in the amount of grafted PEG-anthracene groups was noted to increase the degree of photo-cross-linking upon UV exposure with 60 min of 365 nm light (10 mW/cm<sup>2</sup>) exposure on 80% grafted photogels, resulting in an increase of effective cross-linking density of 39%, whereas 100% grafted photogels resulted in an increase in effective cross-linking density of 105% (data not shown). In addition to having more bound groups to create more cross-linking connections, increases in the amount of PEG-anthracene groups from 80 to 100% likely increases the chance of dimerization to occur since the reaction is dependent on the concentration and density of anthracene groups.<sup>27</sup> Due to their higher sensitivity the 100% (1:1 ratio) grafted gels were used in the loading and release studies.

**Loading and Effective Cross-Linking Density.** For loading and release studies, Coomassie Blue, Fast Green, and dextran were chosen to represent small steroidal drugs and because of their different structures. As illustrated in Table 1, Coomassie Blue and Fast Green are globular and dextran is chain-like. The large proteins, lysozyme, BSA, and myoglobin, were chosen to represent large VEGF-blocker drugs because they are of varying large molecule weights and varying charges at 7.4 due to their different isoelectric points (Table 1). Molecules with isoelectric points above 7.4 are positive in PBS and those with isoelectric points below 7.4 are negative in PBS.

As described in Table 3, loading into un-cross-linked photogels is higher than loading into the tighter, more highly cross-linked control PEG hydrogels. Higher amounts of Coomassie Blue versus Fast Green were loaded into the gels, likely due to charge effects allowing more attraction of Coomassie Blue to the

**Table 3.** Loading of Model Compounds into the Various Types of HA Gels

gel type	model compound	average estimate loading (mg/g gel)
photogels	Coomassie Blue	22.57 ± 2.06
	Fast Green	1.30 ± 0.65
	myoglobin	0.267 ± 0.055 <sup>b</sup>
	lysozyme	0.512 ± 0.138 <sup>a</sup>
	BSA	0.097 ± 0.012 <sup>a</sup>
star-containing photogels	Coomassie Blue	21.92 ± 1.97
control-PEG-hydrogels	Coomassie Blue	1.92 ± 0.11
	myoglobin	0.187 ± 0.043

<sup>a</sup> Loading determined by total release when gel degraded. <sup>b</sup> From Wells et al. 2011.<sup>18</sup>

slightly anionic gels due to its greater ratio of positive groups at pH 7.4 versus Fast Green. Protein loading appears to be dependent on the individual protein properties and relatively efficient. Because the various proteins are approximately 20–80 times larger than Coomassie Blue, it is expected that less protein will load over the same period of time. For example, less BSA is absorbed versus smaller lysozyme over 24 h, likely due to inhibition of absorption of larger BSA. In addition, protein loading may also be somewhat dependent on ionic interactions because BSA is electronegative at the neutral pH of the PBS buffer. Any remaining negative HA carboxyl groups may inhibit absorption, resulting in the observed low loadings. Lysozyme is electropositive at neutral pHs, so its high loading may be partially due to attraction to any remaining HA carboxyl groups. Myoglobin is neutral, therefore, minimal interactions are expected to occur and it loads at amounts between the BSA and lysozyme loadings as expected. Due to detection limits, the loading of dextran could not be determined.

Interactions between HA and loaded compounds could lead to increases in cross-linking. This may be monitored by calculating the effective cross-linking density of loaded versus unloaded photogels and control PEG hydrogels. As illustrated in Figure 2, there were statistically significant increases in effective cross-linking density noted upon the loading of Coomassie Blue into photogels ( $p = 0.0095$ ). Insignificant changes were noted with protein loading (myoglobin  $p = 0.8609$ , lysozyme  $p = 0.0889$ , and BSA  $p = 0.7214$ ) or dextran loading ( $p = 0.8141$ ; single factor Anova) versus unloaded photogels. Therefore, the interactions between Coomassie Blue and the photogels but not the proteins or dextran and the photogels caused physical cross-linking to occur. Control PEG gels are not significantly different upon loading with Coomassie Blue ( $p = 0.0544$ , single factor Anova).

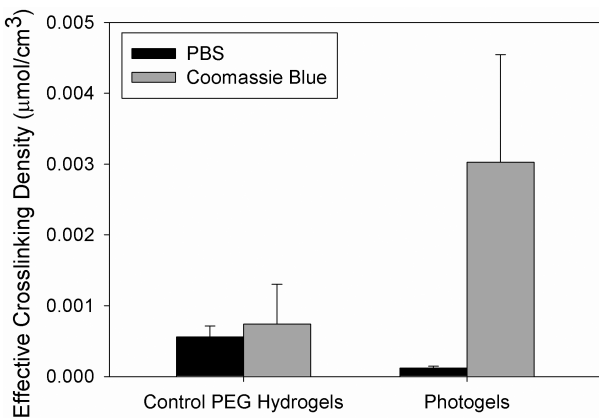


**Figure 2.** Effective cross-linking of unloaded versus loaded photogels and control PEG hydrogels.

Overall, it appears that Coomassie Blue may be interacting with the bound anthracene groups on the HA likely by physical interactions between the aromatic groups present in both molecules. Past studies with alginate photogels also noted potential interactions of Coomassie Blue with both alginate and the anthracene but not in a cross-linking fashion.<sup>28</sup> HA photogels have a PEG-anthracene grafting density that is over 2 times higher than previous alginate photogels. Therefore interactions between the Coomassie blue and the anthracene are more prevalent and affect cross-linking. This will ultimately affect release since the strong interactions will allow for rapid and high loading of Coomassie Blue into the HA photogels but the strong attractions will slow Coomassie Blue diffusion through the gels to allow for controlled release over lengthy periods of time.

**Release of Different Small Model Compounds.** Small model compounds are representative of small drugs such as ophthalmic anti-inflammatory corticosteroids, which are around 500 Da in size.<sup>29</sup> Coomassie Brilliant blue (854 Da), Fast Green (765.89 Da), and dextran (1000 Da) were loaded and released into PBS with either no UV or with UV exposure at 365 nm at 1.5 h for 30 min ( $10 \text{ mW/cm}^2$ ; Figure 3). Irradiation of control solutions of Coomassie Blue and Fast Green in PBS with 365 and 248 nm light did not cause significant changes in their spectrophotometric detection. Dextran, likely due to its linear chain structure and resulting entanglement within the photogel matrix, showed small changes in release after UV treatment whereas globular Coomassie Blue and Fast Green would not entangle and their release was more affected with UV treatment of the photogels.

Early time diffusion coefficients were calculated to observe the influence of the different model compounds on release following UV treatment. Coomassie Blue and Fast Green are quite similar in size and structure with both containing similar numbers of aromatic groups, Coomassie Blue with 6 and Fast Green with 5, that may interact with the anthracene aromatic groups. As shown in Table 4, the percent decrease in the diffusion coefficient upon treatment with 30 min of 365 nm light ( $10 \text{ mw/cm}^2$ ) varied from 62 to 82% between the two molecules. Because there was an undetermined amount of loaded dextran, diffusion coefficients could not be accurately calculated. Both Coomassie Blue and Fast Green interacted with the HA photogels to extend their release although the results suggest that Coomassie Blue was likely more attracted to the HA photogel matrix, indicated by its high loading. Quick loading followed by extended release due to both attractions between the small model drugs and photo-cross-

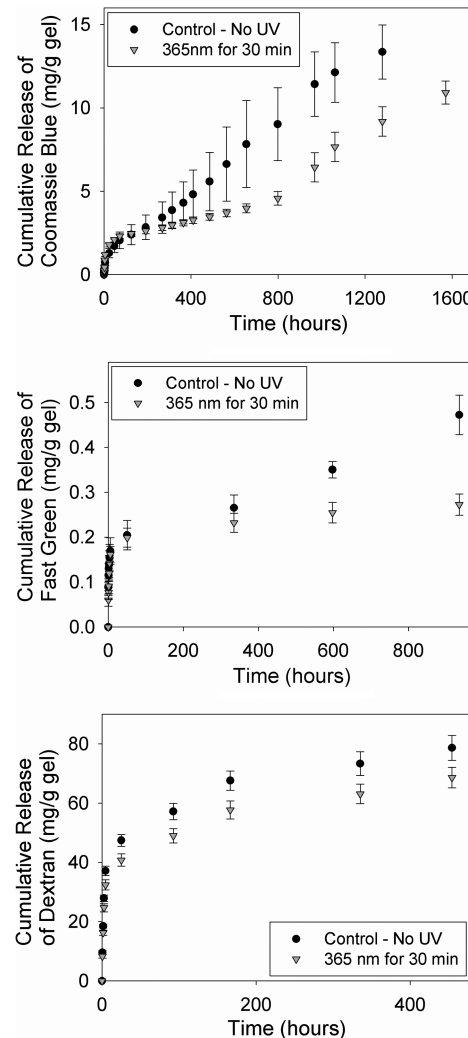


**Figure 3.** Cumulative release of Coomassie Blue, Fast Green, and dextran from HA photogels into PBS at  $37^\circ\text{C}$ . At 1.5 h, one set of gels in each study was treated with 365 nm exposures of  $10 \text{ mW/cm}^2$  for 30 min. Loading of Coomassie Blue was  $22.6 \pm 0.35 \text{ mg/g gel}$ , Fast Green was  $1.3 \pm 0.65 \text{ mg/g gel}$ , and Dextran was undetermined.

linking presents a complex system that provides extended release in a smart stimuli-responsive matrix. Upon close examination, there are two phases of Coomassie Blue release from photo-cross-linked photogels (Figure 3); there is a burst followed by controlled release then a slight second burst followed by controlled release. After 5 mg/g gel has been released a second burst is noted at 800 h. This is thought to be due to a critical concentration of Coomassie Blue being released which lowers the overall cross-linking density of the gels, allowing more dye to escape. Loading at a level below this concentration would prevent a second burst or loadings with compounds that interact in a non-cross-linking fashion would eliminate it entirely.

Early time diffusion coefficients of photogels releasing Coomassie Blue with different UV exposures were compared to determine the effect of different UV treatment times on changes in release rate. As shown in Table 4, increases in 365 nm UV treatment time (exposure) resulted in greater decreases in the diffusion coefficient versus controls. Note that the diffusion coefficients are different due to batch-to-batch variability likely caused by baseline ambient light exposure during synthesis and

**Table 4. Diffusion Coefficients and Exponents for the Release of Fast Green and Coomassie Blue from HA Photogels with Different UV Treatment Times**

model compound	UV time (min)	diffusion coefficient × 10 <sup>11</sup> (cm <sup>2</sup> /s)	diffusion exponents	percent decrease in diffusion coefficient with UV treatment
Fast Green	0	2.87 ± 0.208	0.21 ± 0.07	62%
	30	1.78 ± 0.001	0.09 ± 0.01	
Coomassie Blue	0	5.82 ± 0.028	0.46 ± 0.03	82%
	30	1.06 ± 0.002	0.20 ± 0.01	
Coomassie Blue	0	8.83 ± 0.017	0.51 ± 0.02	66% <sup>a</sup>
	20	2.98 ± 0.011	0.27 ± 0.02	
Coomassie Blue	0	0.49 ± 0.002	0.46 ± 0.03	46%
	7	0.27 ± 0.0003	0.36 ± 0.02	

<sup>a</sup> Calculated from release study in Wells et al. 2011.<sup>18</sup>

processing. Small light exposures in synthesis solutions prior to gel formation, when the photoreaction efficiency is higher, can cause dimerization affecting gel properties. Future use of a dark room during synthesis will prevent unwanted light exposures to reduce the diffusion variability between batches of gels caused by unwanted dimerization/cross-linking. In Vivo, native tissue will filter unwanted UV light to protect photogels from unwanted exposures. Because the photo-cross-linking reaction requires individual absorption of light by anthracene groups increases in UV time increases the amount of dimerization and therefore cross-linking of the HA photogel matrix. The photogels are therefore a unique system with the ability to fine-tune cross-linking and delivery of drug molecules with specified UV treatments. This could have a huge impact in drug delivery technology where current systems are fixed devices assumed to work similarly in different patients. Incremental alterations to fine-tune drug delivery present the opportunity to provide individualized treatments based on the patient and etiology of disease. For retinal drug delivery this is especially important in older populations and diseased eyes. Externally light controlled incremental changes of drug delivery from a device may account for and counterbalance changes that occur in the aging vitreous humor which undergoes liquefaction and contraction ultimately altering drug diffusion and distribution in unpredictable manners.<sup>30</sup>

The addition of star-PEG-anthracene into the HA photogel matrices introduces more anthracene groups for dimerization. As shown in Figure 4, at 400 h there were changes in release of Coomassie Blue from photogels exposed to 20 min of 365 nm light versus controls with no UV light exposures. Changes in release were obvious by 350 h. However, upon close examination, it is apparent that the release rate (slope in Figure 4) decreases in 365 nm treated photogels at 100 h. There was a burst shortly after UV treatments likely since loosely entangled star-PEG-anthracene may cause contraction to temporarily increase release while increasing cross-linking density. This phenomenon was also noted in alginate photogels containing the same star-PEG-anthracene molecule.<sup>28</sup> Overall, the sensitivity of the photogels containing star-PEG-anthracene is higher because large changes in release occurred with 20 min 365 nm UV treatment times, but there is a burst after UV treatment that initially masks this observation.

**Release of Different Large Model Compounds.** Large model compounds are representative of anti-VEGF AMD drug molecules that vary from 48 to 148 kDa in size.<sup>31–34</sup> Lysozyme (14.4 kDa, pI = 9.3) and bovine serum albumin (BSA; 67 kDa,

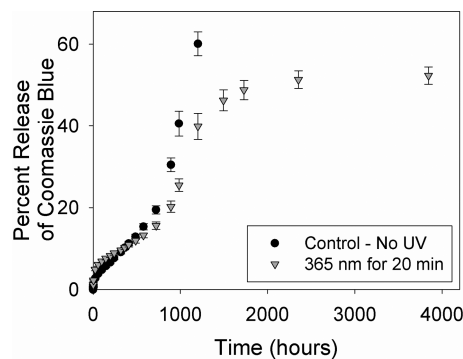


**Figure 4.** Cumulative release of Coomassie Blue from star-PEG-anthracene containing HA photogels into PBS at 37 °C. At 1.5 h, one set of gels was treated with 365 nm exposures of 10 mW/cm<sup>2</sup> for 20 min. Loading of Coomassie Blue was 21.9 ± 1.9 mg/g gel.

pI = 4.9) release show an “off effect” when the photogels are irradiated with 365 nm light for 30 min (10 mW/cm<sup>2</sup>, total fluence of 18000 mJ/cm<sup>2</sup>; Figure 5). This is consistent with previous studies by Wells et al. 2010, which demonstrated myoglobin (17.6 kDa pI = 7.3, minor 6.8) release from HA photogels that could be turned off with similar exposures.<sup>18</sup> The effect is attributed to the increased cross-linking density greatly inhibiting the diffusion of the large proteins. Control studies of proteins in PBS exposed to UV light showed no changes in their spectrophotometric detection. Despite differences in molecular weight and charge of BSA, lysozyme, and myoglobin, 365 nm treatment of the HA photogels sufficiently shut release down, suggesting a size rather than a charge effect and indicating that the system is versatile and will work with a multitude of different large molecular weight drugs. The “off effect” noted with 365 nm exposures was found to occur even with low 365 nm exposures. Specifically 10 min of 365 nm light (10 mW/cm<sup>2</sup>) was sufficient to stop the release of myoglobin from the photogels (data not shown).

The initial burst from photogels releasing BSA and lysozyme is 44 and 42% of their loaded protein before 365 nm UV exposure shuts down release. In PBS of pH 7.4, it would be expected that slightly negative BSA due to its low pI would burst and release quickly from slightly negative HA but instead it releases similarly to slightly positive lysozyme. With photo-cross-linking, it also releases over a relatively lengthy time extending past 2.5 months. Interestingly, past studies have shown some interaction exists

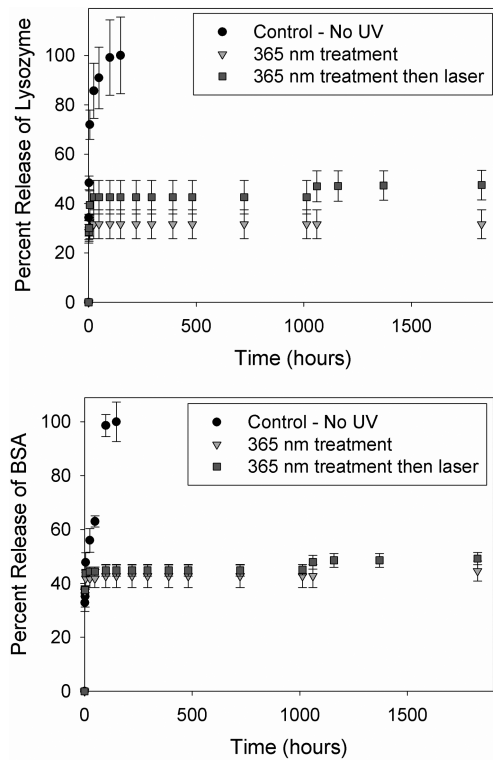


**Figure 5.** Lysozyme and BSA release from photogels. At 2 h, two sets of gels were irradiated with 365 nm at  $10 \text{ mW/cm}^2$  for 30 min ( $18000 \text{ mJ/cm}^2$ ). At 1038 h, one set of gels was then exposed to a 248 nm excimer laser for  $18000 \text{ mJ/cm}^2$  (310 pulses of  $58 \text{ mJ/cm}^2$  at 5 Hz). Loading of lysozyme was  $0.512 \pm 0.14 \text{ mg/g}$  gel and of BSA was  $0.097 \pm 0.01 \text{ mg/g}$  gel.

between anthracene derivatives and human serum albumin.<sup>35</sup> Therefore, it is possible that these interactions contribute to the lengthy release time of BSA from the photogels despite its low loading and attraction. Lysozyme, which is slightly positive at pH 7.4 due to its high pI, should show a small attraction to the HA photogels. Therefore, more lysozyme loaded into the gels but showed slower release than BSA from laser treated photo-cross-linked photogels.

When photogels were exposed to a 248 nm excimer laser for  $18000 \text{ mJ/cm}^2$  (310 pulses of  $58 \text{ mJ/cm}^2$  at 5 Hz) the protein release turned back on (Figure 5). There was a slight burst followed by little to no protein release. De-cross-linking from 248 nm is caused by anthracene dedimerization/dissociation at the surface of the photogels to increase release and the laser exposure was matched to be equivalent to the 365 nm light that previously shut release off. The small increase in protein release with 248 nm laser exposure is thought to occur because the surface and not the bulk of the photogels were de-cross-linked because HA effectively absorbs UV at 248 nm to prevent its penetration into the photogels, as illustrate in previous studies by Wells et al.<sup>18</sup>

Diffusion coefficients were used to compare and assess the recovery in release that occurred when the release of protein from photogels was shut down by 365 nm light then turned back on by 248 nm laser treatments. Table 5 shows the diffusion coefficients before and after 365 nm light and 248 nm laser treatments. Following laser exposure, lysozyme release turned on and had continual release for 146 h with a 2.6% recovery in the diffusion coefficient. With the laser treatments, BSA release from

photogels had an 18.4% recovery of the diffusion coefficient for 146 min then release stopped. The negative charge of BSA at pH 7.4 may cause a quick release of protein at the surface that escapes after laser exposure, an effect presumably overcome in the lysozyme containing gels which are likely attracted to the HA matrix.

The use of the 248 nm excimer laser demonstrates the proof of concept for the photogels as an ophthalmic device that may be stimulated with lasers. High wavelengths are well-used and known to penetrate the eye and low wavelengths are known to penetrate when above  $600 \text{ mW/cm}^2$ .<sup>36</sup> However, two-photon absorption (TPA) may offer a safer opportunity to cause effective dimerization and dedimerization at the back of the eye. Ocular tissues at the front of the eye may absorb UV.<sup>37</sup> TPA uses high wavelength visible light that can penetrate through the cornea and lens to accumulate at the required UV wavelengths with high dimensional and spatial selectivity.<sup>38</sup> Importantly, TPA has been demonstrated to deliver low UV wavelengths and, for example, has effectively caused the dissociation of the photodimerizing molecule coumarin.<sup>39</sup> TPA may also allow deeper penetration of UV  $< 300 \text{ nm}$  into the HA photogels. The 248 nm excimer laser exposure could not penetrate the HA photogels resulting de-cross-linking at the surface to produce small increases in release seen at 1000 h in Figure 5. Exposures using TPA may result in deeper penetration into the photogels to cause bulk de-cross-linking and therefore greater changes in release.

The trends between the different types of proteins show the ability for the photogels to control their release and increase or decrease their release under specific conditions of UV exposure. Wet AMD anti-VEGF drugs have various properties and are around 48–148 kDa in size. Therefore these HA photogels provide a workable platform for their long-term, photocontrollable delivery. By lowering the 365 nm photo-cross-linking UV exposures, tunable release profiles similar to those seen with Coomassie Blue release, should be obtainable to allow continuous large molecule release. In addition, the ability to turn off release is a critical asset for patients with adverse side effects to drugs being delivered by intravitreal drug delivery devices and could be incorporated into existing devices as a new safety mechanism to allow quick and easy shutdown of drug release when adverse reactions occur.

**Gel Degradation.** When placed *In Vivo*, HA gels may degrade by the enzyme hyaluronidase (HAase), which is present in the posterior segment of the eye at 20 turbidity reducing units (TRU) per mL in human vitreous humor.<sup>40</sup> Both hydrolytic/de-cross-linking degradation that may occur in aqueous solutions such as PBS and enzymatic degradation in solutions of HAase were determined to be related to covalent modifications of HA with PEG and to UV cross-linking. HAase concentrations of 100 units/mL were used to speed up observed effects. Photogel degradation rates were decreased after UV cross-linking treatments of 30 min at 365 nm ( $10 \text{ mW/cm}^2$ ) from degradation in approximately 400 h to past 3000 h in PBS and from 48 h to past 440 h in 100 units/mL of hyaluronidase. While control PEG hydrogels were found to last over 800 h in PBS, HAase caused degradation times to decrease to  $\sim 220$  h both with and without UV exposure, consistent with literature,<sup>41</sup> illustrating the lack of UV effect on the HA control hydrogels. As expected, the increased degradation times of the HA photogels in PBS and with HAase was dependent on their cross-linking density from 365 nm UV exposure. HAase is a relatively large enzyme composed of 4 units of 14 kDa,<sup>42</sup> which must diffuse into the

**Table 5.** Diffusion Coefficients and Exponents for the Release of Proteins from HA Photogels before and after 365 nm Light and 248 nm Laser Treatments

protein	treatment	diffusion coefficient ( $\text{cm}^2/\text{s}$ )	diffusional exponent	percent recovery of the diffusion coefficient with laser exposure on 365 nm photo-cross-linked gels
lysozyme	no UV (control)	$7.15 \times 10^{-10}$	0.15	2.6%
	after 365	0	0	
	after 365 and laser	$1.84 \times 10^{-11}$	0.22	
	after 146 min (post-laser)	$4.63 \times 10^{-13}$	0.01	
BSA	no UV (control)	$5.88 \times 10^{-10}$	0.12	18.4%
	after 365	0	0.003	
	after 365 and laser	$1.08 \times 10^{-10}$	0.5	
	after 146 min (post-laser)	0	0	

gels to effectively cause degradation. Therefore, photo-cross-linking slows the influx of the enzyme, thereby inhibiting enzymatic biodegradation.

Of note are the long hydrolytic/de-cross-linking degradation times associated upon the loading and release of Coomassie Blue and Fast Green into PBS from photogels that have no 365 nm photo-cross-linking UV. Loading of Coomassie Blue increased control photogel (no UV) degradation from approximately 400 h to over 1000 h in PBS and is attributed to interactions between the dye and the photogels. Fast Green loading had a similar effect increasing degradation past 800 h with control photogels (no UV). This observation is not noted with photogels loaded with proteins (myoglobin, lysozyme and BSA) suggesting some cross-linking interactions between the Coomassie Blue and the photogels but not between the proteins and the photogels. Since spectrophotometric studies did not indicate that that UV treatment resulted in covalent interactions between Coomassie Blue and anthracene, it is likely that the interactions are physical, allowing for a slowed and lengthy release and reduced photogel degradation. This is consistent with the observations that Coomassie Blue increased the effective cross-linking density of the photogels (Figure 2) and together they prove there is physical cross-linking occurring. HAase present In Vivo will ultimately influence release of drugs from the photogels but minimally when they are photo-cross-linked. The amounts will be lower than 100 unit/mL and will likely vary between different patients but this degradation can be accounted for by fine-tuning photogel properties by appropriate UV light treatment of the gel to dial in specific drug release rates.

**Cytocompatibility Studies.** Preliminary studies have shown that human corneal epithelial cells are viable with HA and alginate photogels.<sup>18</sup> However, human RPE cells better represent the posterior segment of the eye so were used for a thorough investigation into HA photogel cytocompatibility.

Cells were grown with solutions of PEG-anthracene cross-linker to evaluate its direct effect on cells. Initial screening assays demonstrated that concentrations around 0.1 mg/mL negatively impacted cell growth. Therefore, cells at different densities were grown at concentrations between 0 and 0.7 mg/mL over 3 and 7 days. As shown in Figure 6, higher cell concentrations were least affected by PEG-anthracene, with seeding densities over 34000 cells/well having normal growth up to concentrations of 0.1 mg/mL. Lower cell seeding concentrations of 17000 cells/well with PEG-anthracene concentrations over 0.05 mg/mL had negatively impacted growth. In Vivo, it is expected that very little unbound PEG-anthracene will be present since very little is detected after the gels are soaked in water for 24 h after synthesis.

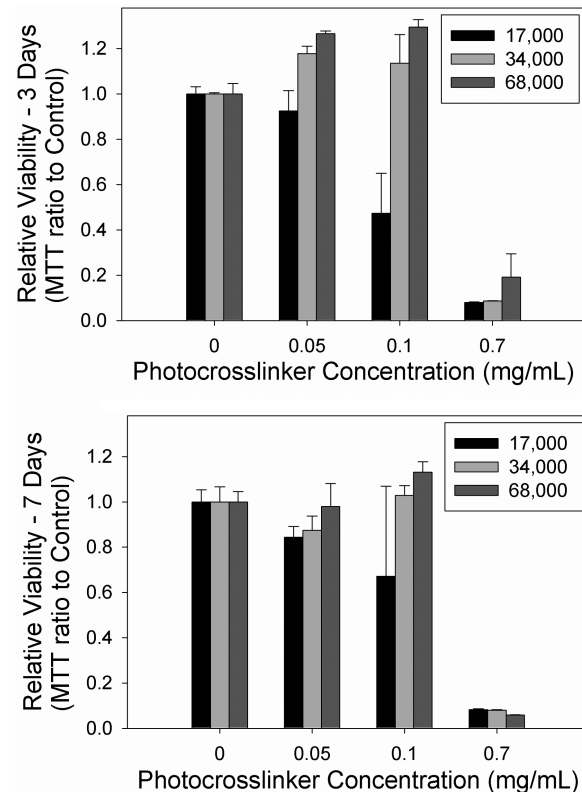


**Figure 6.** MTT assay results of RPE cells growth with varying PEG-anthracene concentrations over 3 and 7 days.

A 1 mm thick and 0.5 cm diameter gel, such as those that were used for drug release studies, contains  $5.86 \pm 0.02 \mu\text{g}$  unbound anthracene per disk. In addition there is approximately 1.32 mg of bound PEG-anthracene per disk that is not likely to be released because covalently bound. The gel sizes are much larger than those that would be used In Vivo as compared to other release devices on the market, so once sized appropriately for In Vivo applications, even less PEG-anthracene would be present.<sup>43</sup>

Also important is the potential effect solutions of HA have on cell growth. HA is well-known to affect cell behavior, including adhesion, migration, and proliferation. RPE cells have been shown to produce HA and maybe be affected by HA via binding to CD44 receptors.<sup>44</sup> Minimal changes in growth were noted when RPE cells were grown in 0.01 and 0.1 mg/mL HA in medium versus controls grown in medium (data not shown). Therefore, the bulk HA of the photogels is not expected to

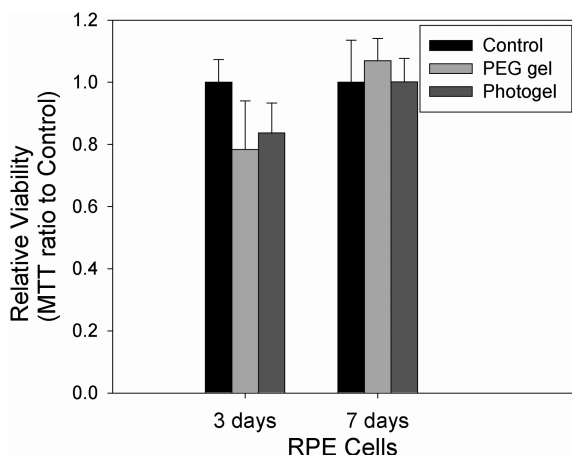


**Figure 7.** Gels were added to a confluent layer of RPE cells after 24 h of growth. After 3 and 7 days there were no significant changes in growth between the PEG gels and the controls (3 days,  $p = 0.696$ ; 7 days,  $p = 0.148$ ) and between the photogels and the controls (3 days,  $p = 0.998$ ; 7 days,  $p = 0.414$ ) when evaluated using the MTT assay and single factor anova.

significantly increase cell growth. Since present PEG-anthracene will be bound to HA polymer chains, RPE cells grown with gels and degradation products were also investigated because they are more representative of In Vivo systems.

**Cell Grown in Indirect Contact.** Cells grown in the presence of gels evaluate the effect of any released short-term degradation and side products on cell viability. In all cases, both the control PEG hydrogels (3 days,  $p = 0.696$ ; 7 days,  $p = 0.148$ ) and the photogels (3 days,  $p = 0.998$ ; 7 days,  $p = 0.414$ ) did not cause significant changes in growth in RPE cells versus controls, as illustrated in Figure 7. RPE cells grown with control PEG gels and photogels had similar growth and respiration over 3 and 7 days, showing the relative cytocompatibility of the photogels. Any leftover byproduct does not significantly effect cell growth, and binding of PEG-anthracene to HA protects cells from its effects. Future studies will check the effects of UV because gels should provide a protective barrier if grown between the UV source and the cells.

**Long-Term Degradation Product Study.** With long-term implantations, released degradation products are a concern for cell toxicity. Therefore, medium used to soak gels for 45 days were grown with cells to evaluate the possible effect of long-term degradation products on cell cytocompatibility. This was compared to medium that was under the same conditions for 45 days as well as a control of fresh medium. There were no significant changes in growth with RPE cells grown with low ( $p = 0.343$ ) or high ( $p = 0.896$ ) concentrations of degradation products versus medium, as shown in Figure 8.

As the photogels degrade, the risk that PEG-anthracene might leach out increases. However, after 45 days, this risk appears minimal, demonstrated from the lack of changes in cell growth. Degradation products are not expected to build up to high concentrations In Vivo due to their local transport and removal. Even so, high concentrations were not shown to significantly impact RPE cell viability and even less effects were noted with the more representative low concentrations of degradation products. While showing high compatibility with RPE cells, further cytocompatibility studies and ultimately In Vivo studies will be required in the future.

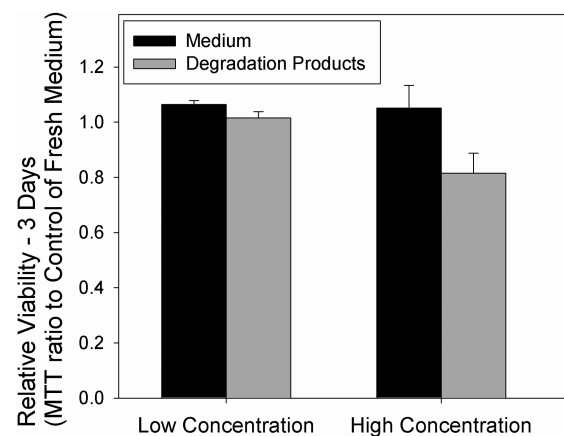


**Figure 8.** Confluent layers of RPE cells had no changes in growth when exposed to media containing low concentrations of degradation products versus controls of medium ( $n = 4$ ,  $p = 0.343$ ) or high concentrations of degradation products versus controls of medium ( $n = 4$ ,  $p = 0.896$ ) when evaluated using the MTT assay and single factor anova.

## CONCLUSIONS

The HA photogels have the potential to act as controlled long-term delivery materials, showing photoresponsive changes in the release of small and large molecular weight model drug compounds that represent steroid and wet-AMD drugs. Release can be slowed in an incremental fashion or turned off completely, dependent on UV exposures and the size of the model drugs. HA photogels show high compatibility with human retinal cell lines, demonstrating their potential capability for drug delivery In Vivo. Once put into an appropriate platform, these materials can be used to control release rates, to shut-down the release of drugs if adverse reactions occur, and to tailor drug delivery to the patient and disease over the long-term.

## AUTHOR INFORMATION

### Corresponding Author

\*Phone: 905-525-9140, ext. 24794. Fax: 905-521-1350. E-mail: sheardow@mcmaster.ca.

## ACKNOWLEDGMENT

Funding support from NSERC and 20/20 NSERC Ophthalmic Materials Network is gratefully acknowledged. Dr. John Preston and Gabriel Devenyi are acknowledged for excimer laser expertise.

## REFERENCES

- (1) Qiu, Y.; Park, K. *Adv. Drug Delivery Rev.* **2001**, *53*, 321–339.
- (2) Molokhia, S. A.; Sant, H.; Simonis, J.; Bishop, C. J.; Burr, R. M.; Gale, B. K.; Ambati, B. K. *Vision Res.* **2010**, *50*, 680–685.
- (3) Lang, J. C. *Adv. Drug Delivery Rev.* **1995**, *16*, 39–43.
- (4) Urtti, A. *Adv. Drug Delivery Rev.* **2006**, *58*, 1131–1135.
- (5) del Amo, E. M.; Urtti, A. *Drug Discovery Today* **2008**, *13*, 135–143.
- (6) Kurz, D.; Ciulla, T. A. *Ophthalmol. Clin. North Am.* **2002**, *15*, 405–410.
- (7) Fletcher, E. C.; Lade, R. J.; Adewoyin, T.; Chong, N. V. *Ophthalmology* **2008**, *115*, 2192–2198.
- (8) Yasukawa, T.; Ogura, Y.; Tabata, Y.; Kimura, H.; Wiedemann, P.; Honda, Y. *Prog. Retinal Eye Res.* **2004**, *23*, 253–281.

- (9) Booth, B. A.; Denham, L. V.; Bouhanik, S.; Jacob, J. T.; Hill, J. M. *Drugs Aging* **2007**, *24*, 581–602.
- (10) Yasukawa, T.; Ogura, Y.; Sakurai, E.; Tabata, Y.; Kimura, H. *Adv. Drug Delivery Rev.* **2005**, *57*, 2033–2046.
- (11) Choonara, Y. E.; Pillay, V.; Danckwerts, M. P.; Carmichael, T. R. d. L.C. *J. Pharm. Sci.* **2010**, *99*, 2219–2239.
- (12) Holz, F. G.; Korobelnik, J.; Lanzetta, P.; Mitchell, P.; Schmidt-Erfurth, U.; Wolf, S.; Markabi, S.; Schmidli, H.; Weichselberger, A. *Invest. Ophthalmol. Visual Sci.* **2010**, *51*, 405–412.
- (13) Lalwani, G. A.; Rosenfeld, P. J.; Fung, A. E.; Dubovy, S. R.; Michels, S.; Feuer, W.; Davis, J. L.; Flynn Jr., H. W.; Esquiabro, M. *Am. J. Ophthalmol.* **2009**, *148*, 43–58.e1.
- (14) Bouas-Laurent, H.; Castellan, A.; Desvergne, J. D.; Lapouyade, R. *Chem. Soc. Rev.* **2001**, *30*, 248–263.
- (15) Kumar, G. S.; Neckers, D. C. *Chem. Rev.* **1989**, *89*, 1915–1925.
- (16) Kaur, M.; Srivastava, A. K. *J. Macromol. Sci., Polym. Rev.* **2002**, *C42*, 481–512.
- (17) Bishop, P. N. *Prog. Retinal Eye Res.* **2000**, *19*, 323–344.
- (18) Wells, L. A.; Brook, M. A.; Sheardown, H. *Macromol. Biosci.* **2011**, submitted for publication.
- (19) Bray, J. C.; Merrill, E. W. *J. Appl. Polym. Sci.* **1973**, *17*, 3779–3794.
- (20) Flory, P. J.; Rehner, J. *J. Chem. Phys.* **1943**, *11*, 521–526.
- (21) de Jong, S. J.; van Eerdernbrugh, B.; van Nostrum, C. F.; Kettenes-van den Bosch, J. J.; Hennink, W. E. *J. Controlled Release* **2001**, *71*, 261–275.
- (22) Leach, J. B.; Bivens, K. A.; Patrick, C. W.; Schmidt, C. E. *Biotechnol. Bioeng.* **2003**, *82*, 578–589.
- (23) Li, C. Y.; Birnkranz, M. J.; Natarajan, L. V.; Tondiglia, V. P.; Lloyd, P. F.; Sutherland, R. L.; Bunning, T. J. *Soft Matter* **2005**, *1*, 238–242.
- (24) Leach, J. B.; Schmidt, C. E. *Biomaterials* **2005**, *26*, 125–135.
- (25) Chorny, R. C.; Krasuk, J. H. *Ind. Eng. Chem. Proc. Des. Dev.* **1966**, *5*, 206–208.
- (26) Ritger, P. L.; Peppas, N. A. *J. Controlled Release* **1987**, *5*, 23–36.
- (27) Bratschkov, C.; Karpuzova, P.; Mullen, K.; Klapper, M. *Polym. Bull.* **2001**, *46*, 345–349.
- (28) Wells, L. A.; Sheardown, H. *Eur. J. Pharm. Biopharm.* **2011**, submitted for publication.
- (29) Jaffe, G. J.; Ashton, P.; Pearson, P. A. *Intraocular Drug Delivery*; Taylor and Francis: New York, 2006.
- (30) Laude, A.; Tan, L. E.; Wilson, C. G.; Lascaratos, G.; Elashry, M.; Aslam, T.; Patton, N.; Dhillon, B. *Prog. Retinal Eye Res.* **2010**, *29*, 466–475.
- (31) Blick, S. K. A.; Keating, G. M.; Wagstaff, A. J. *Drugs* **2007**, *67*, 1199–1206.
- (32) Ahmadi, M. A.; Lim, J. I. *Expert Opin. Pharmacother.* **2008**, *9*, 3045–3052.
- (33) Landa, G.; Amde, W.; Doshi, V.; Ali, A.; McGevna, L.; Gentile, R. C.; Muldoon, T. O.; Walsh, J. B.; Rosen, R. B. *Ophthalmologica* **2008**, *223*, 370–375.
- (34) Anderson, O. A.; Bainbridge, J. W. B.; Shima, D. T. *Drug Discovery Today* **2010**, *15*, 272–282.
- (35) Skupinska, K.; Zylm, M.; Misiewicz, I.; Kasprzycka-Guttman, T. *Acta Biochim. Pol.* **2006**, *53*, 101–112.
- (36) Schmidt-Erfurth, U.; Hasan, T. *Surv. Ophthalmol.* **2000**, *45*, 195–213.
- (37) Thompson, K. P.; Ren, Q. S.; Parel, J. M. *Proc. IEEE* **1992**, *80*, 838–860.
- (38) Bhawalkar, J. D.; He, G. S.; Prasad, P. N. *Rep. Prog. Phys.* **1996**, *59*, 1041–1070.
- (39) Hartner, S.; Kim, H. C.; Hampp, N. *J. Polym. Sci., Part A: Polym. Chem.* **2007**, *45*, 2443–2452.
- (40) Schwartz, D. M.; Shuster, S.; Jumper, M. D.; Chang, A.; Stern, R. *Curr. Eye Res.* **1996**, *15*, 1156–1162.
- (41) Jeon, O.; Song, S. J.; Lee, K. J.; Park, M. H.; Lee, S. H.; Hahn, S. K.; Kim, S.; Kim, B. - *Carbohydr. Polym.* **2007**, *70*, 251–257.
- (42) Khorlin, A. Y.; Vikha, I. V.; Milishnikov, A. N. *FEBS Lett.* **1973**, *31*, 107–110.
- (43) Weiner, A. Drug delivery systems in ophthalmic applications. In *Ocular Therapeutics: Eye on New Discoveries*; Yorio, T., Clark, A. F., Wax, M. B., Eds.; Academic Press: New York, 2008; pp 7–30.
- (44) Garg, H. G.; Hales, C. A. *Chemistry and Biology of Hyaluronan*; Elsevier Ltd.: Oxford, U.K., 2004.